PULLOUT LOAD ANALYSIS OF REINFORCE CONCRETE ANCHOR SHAFTS

H. Haji-Kazemi

Department of Civil Engineering
Ferdowsi University of Mashhad
Mashhad, Iran

Abstract In this paper, results obtained in both conventional and finite element analysis of straight and belled anchor shafts subjected to a pullout force are presented. In numerical analysis, it is assumed that no drainage takes place during the anchor pullout. Comparisons between two conventional methods of analysis for ultimate pullout load and the results obtained by the finite element analysis are also presented. The load-deformation and stress-strain responses in the shaft, in the interface between shaft and soil, as well as in the soil are discussed.

Key Words Anchors, Straight Belled, Pullout Louds, Concrete, Soil, Soil-Structure Interaction Deformations, Finite Elements

چکیده در مقاله زیر نتایج حاصل از آنالیز قلاب های استوانه ای و مخروطی شکل که تحت اثر بارهای کششی قرار گرفته باشند به روش اجزاء محدود و روش های مرسوم ارائه شده است. در آنالیز عددی فرض براین است که زهکشی انجام نمی شود. مقایسه بین دو روش مرسوم و روش اجزاء محدود پیشنهادی نیز ارائه گردیده و اثرات بار-تغییر مکان و تنش-کرنش در قلاب، درحد فاصل بین خاک و قلاب و خاک مورد بحث و بررسی قرار گرفته است.

INTRODUCTION

Offshore structures, bridge, dams, tower footing, high-rise buildings and other surface structures are subjected to forces caused by wind, waves, earthquakes, dead load of the structure, etc. Wind and wave forces are predominately of a horizontal nature, and they tend to overturn the structures, which in turn can result in uplift and lateral movements of the foundations. These types of structures are considered more likely to fail when subjected to upward or lateral forces rather than gravity-induced downward forces.

In order to prevent failures caused by lateral and uplift forces, the structure has to be connected to other geologic formations that are far stiffer and stronger than the medium in immediate contact with the man-made facilities. This can be achieved by means of anchoring.

The main objective of this paper is to study the pullout strength and deformational behaviour of anchor shafts. At present no generally accepted method exists for calculating soil uplift resistance or deformation due to tensile foundation forces.

The investigation presented here is concerned with: 1-the behaviour of straight and belled reinforced concrete anchor shafts subjected to pullout forces, 2-the stress distribution in the soil around the shaft during loading, 3-the variation of stresses in the soil and the interface of shaft and soil with respect to depth, and 4-the load-displacement response of the shaft and soil.

For the purpose of this study two different shapes of concrete footing as shown in Figure 1 are chosen.

The uplift load capacity of the model anchors are computed by conventional limit equilibrium and finite element methods of analysis. These methods are currently used by engineers for pullout analysis.

Since the finite element method (FEM) is one of the most versatile procedures available, major attention is devoted to this scheme.

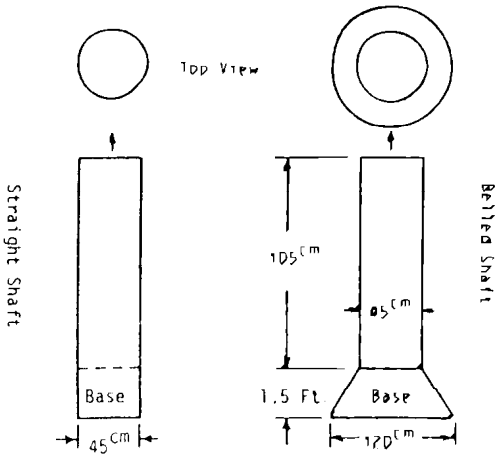

Figure 1. Model anchors

MATERIALS

In order to use closed form and analytical schemes to simulate the soil structure interaction behaviour of an anchor shaft in soil under tension, relevant material properties are needed.

The material used for anchor shafts is reinforced concrete. It is assumed that the material behaves linearly elastic and does not exceed is ultimate compressive strength. Shaft material possesses the following properties:

Compressive strength	$f'_c = 2000$ N/cm^2
Young's modulus	$E_c = 2.07 \times 10^6$ N/cm^2
Unit weight	$\gamma_c = 2.35 \times 10^{-2}$ N/cm^3
Poison ratio	$\nu_c = 0.32$

The anchor is assumed embedded in Boston Blue Clay. This soil has been investigated thoroughly and the indices and parameters describing the soil are readily available in the literature [1]. Results of consolidated undrained plane strain active and passive tests are available for samples of remoulded speciments at over consolidation ratios (OCR) of 1,2 and 4. Test data show that Boston Blue Clay has highly anisotropic undrained properties. It has a specific gravity of 2.79, and contains approximately 50% clay size material. The typical index properties of the clay used in this study are:

Water content	36 ± 2%
Liquied limit	41 ± 2%
Plastic limit	20 ± 2%
plasticity index	21 ± 3%

The coefficient of earth pressure at rest, K_0 for these three over consolidation ratios, and stiffness parameters of the soil are given in Table 1. The drained internal angle of friction of the soil is measured to be $\phi_d = 30°$, and the undrained internal angle of friction, ϕ_{ud} is 5°.

TABLE 1. OCR vs. K_o and Stiffness Parameters of Boston Blue Clay

OCR	K_0	σ_3, N/cm^2	E_i, N/cm^2
1	0.55	3.0	56.0
2	0.73	8.8	162.8
4	0.89	20.9	210.0

FINITE ELEMENT ANALYSIS

The soil-anchor interaction problem under study is concerned with stresses and deformations in the soil due to boundary traction and body forces. In the finite element method, the soil mass is assumed to consist of a finite number of discrete elements interconnected at a finite number of nodal points. The geometric and material properties of each element are such that the assemblage of elements behaves in a manner similar to that of the orginal continuum.

In the finite element modelling, the continua, that is soil and structure are discretized into two-dimensional quadrilateral elements as shown in Figure 2(a). The displacement components u and v at a point within each element can be expressed as

$$\{u\ v\}^T = \{U\} = [N].\{q\}$$

where $\{U\}$ is the vector of displacements at a point, $[N]$ is the matrix of interpolation function, and $\{q\}$ is the vector of displacements at element nodes which is

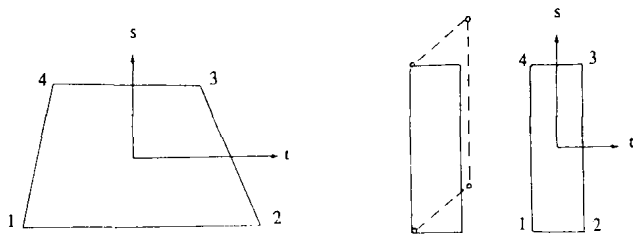

Figure 2. (a) Quadrilateral element ; (b) Joint interface

$$\{q\}^T = [u_1\ v_1\ u_2\ v_2\ u_3\ v_3\ u_4\ v_4]$$

The behaviour at a junction between structure and soil can be simulated by discretizing it by using an interface or joint element. The interface element shown in Figure 2(b) permits relative movement between two adjacent nodes, and computational difficulties are avoided by using forces and relative displacements as state variables. A detailed discussion of the interface or joint element is given by Goodman *et al.* [4].

Variational or residual procedures can now be used for evaluating the element stiffness equations using the principle of stationary potential energy with axisymmetric idealization and linear elastic behaviour of material.

After deriving the equations for the interface elements, the joint stiffness matrix can be written as:

$$[K] = \int_l [B]^T [C]\ [B]\ dl$$

where L is the coordinate along the element length, [B] is the relative nodal displacement transformation matrix and [C] is the interface element stiffness or constitutive matrix given by:

$$[C] = \begin{bmatrix} k_{ss} & k_{sn} \\ k_{ns} & k_{nn} \end{bmatrix}$$

k_{ss}, k_{nn} and $k_{sn} = k_{ns}$ are stiffness coefficients in shear, normal and cross shear-normal directions respectively.

To represent the problem realistically, some form of non-linear stress-strain relation must be used. For defining the constitutive behaviour of soil, the hyperblic Duncan-Cheng model [5] has been used here in order to simulate the soil and soil-structure interface stress-strain or relative deformation behaviour.

The stress-strain curves for the clay is approximated as hyperbolas with the relation expressed as:

$$(\sigma_1 - \sigma_3) = \varepsilon / (a + b.\varepsilon)$$

where σ_1 and σ_3 are major and minor principle stresses respectively, $\varepsilon = \varepsilon_1 - \varepsilon_3$ is the axial strain, a is the reciprocal of the initial tangent modulus, and b is the reciprocal of the asymptotic value of stress difference $(\sigma_1 - \sigma_3)_{ult}$, the value at which the stress-strain curve approaches infinite strain (Figure 3(a)).

The value of a and b can readily be determined if the stress-strain data are plotted on the transferred axis shown in Figure 3(b), and the equation can be written as:

$$\varepsilon / (\sigma_1 - \sigma_3) = a + b.\varepsilon$$

It is often found that the asymptotic value of $(\sigma_1 - \sigma_3)$ is larger than the compressive strength of the soil by a small amount [5]. This could be expected, because the hyperbola frequently remains below the asymptote for all the values of strains. To overcome this difficulty, the asymptotic value can be expressed by the compressive triaxial strength using a factor R_f such that

$$(\sigma_1 - \sigma_3)_f = R_f\ (\sigma_1 - \sigma_3)_{ult}$$

where $(\sigma_1 - \sigma_3)_f$ = compressive strength at failure

$(\sigma_1 - \sigma_3)_{ult} = 1/b$ = the asymptotic value of stress difference

R_f = failure ration (less than 1)

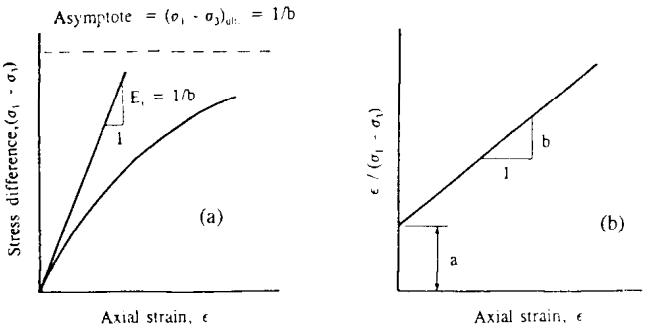

Figure 3(a). Hyperbolic stress-strain curve
Figure 3(b). Transformed hyperbolic stress-strain curve

By expressing a and b in terms of the initial modulus and the compressive strength, the hyperbolic relationship becomes

$$(\sigma_1 - \sigma_3) = \varepsilon / [\frac{1}{E_i} + \frac{\varepsilon R_f}{(\sigma_1 - \sigma_3)_f}]$$

Experimental studies have shown that Ei can be expressed as a function of σ_3 by the following relationship:

$$E_i = KP_a \left(\frac{\sigma_3}{p}\right)^n$$

where K is a modulus, P_a is atmospheric pressure and n is an exponent determining the rate of variation of E_i.

The relationship between compressive strength and confining pressure can be expressed in terms of Mohr-Coulomb failure theory, in which case the expression for the tangent modulus E_t is

$$E_t = KP_a \left(\frac{\sigma_3}{p_a}\right)^n \left[1 - \frac{R_f (1 - \sin\phi)(\sigma_1 - \sigma_3)}{2C\cos\phi + 2\sigma_3 \sin\phi}\right]^2$$

The interface's hyperbolic constitutive relation is given as:

$$K_{st} = COEF\ \gamma_w \left(\frac{\sigma_n}{p_a}\right)^n [1 - (\frac{R_f \tau}{C_a + \tau_n \tan\delta})^2]$$

where COEF is a modulus, σ_n is normal stress at interface, τ is shear stress, C_a is adhesion and d is interface friction.

The basic variables considered to be relevant in the soil-structure systems are as follows:

P = applied load
L= length of shaft
r= radius of shaft
E_c= Young's modulus of shaft material
G_s= shear modulus of soil
ν_s= Poisson's ratio of soil
C= Cohesion
ϕ= angle of internal friction
z,v,y= deformation of shaft and soil

Therefore: y= f (P, L, r, E_c, G_s, V_s, ϕ, c, R_f, σ_1, σ_3, etc.).

The computer program developed by the author for this study is based on the stiffness formulation of the finite element described above. The finite element mesh consists of 331 element for the straight shaft, and 337 elements for the belled shaft. A rigid boundary is imposed at a depth of 3.6 m, and a rigid vertical boundary is prescribed at a horizontal distance of 3.0 m from the centre line of the shaft. This is illustrated in Figure 4. Due to the symmetry of the shaft and soil, one side of the model is considered only.

The input material parameters for the problem under consideration are:

Soil

The soil parameters used in the analysis are the results of tests on undrained specimens and are as follows: $E_s = 56.3$ N/cm^2, $\nu_s = 0.48$, $\gamma_s = 2.35 \times 10^{-2}$ N/cm^3, $R_f = 0.8$, K-loading= K-unloading= 150, c= 4.79 N/cm2, friction angle ϕ= 5°, and the exponent n=0.

Structure

The shaft's material parameters are: 2.07×10^6 N/cm^2, $\nu_c = 0.32$, $\gamma_c = 2.35 \times 10^{-2}$ N/cm^3, K-loading= K-unloading= 0, and the coefficient of earth pressure at rest K_0 has been taken as 0.95.

Interface

Interface residual shear stiffness $k_{ss} = 0.48$ N/cm^2, adhesion $C_a = 3.83$, angle of friction ϕ= 4°, $R_f = 0.8$, exponent n= 0, and K-loading= 10^7 for the results shown in Figures 5 through 9.

RESULTS

In order to evaluate the sensitivity of K-loading (COEF) and its influence on the interface element's behaviour, a set of trial and error analyses were performed until a realistic value was reached. By decreasing the value of K, it was observed that the load-displacement curve became steeper and finally the load capacity for both straight and belled

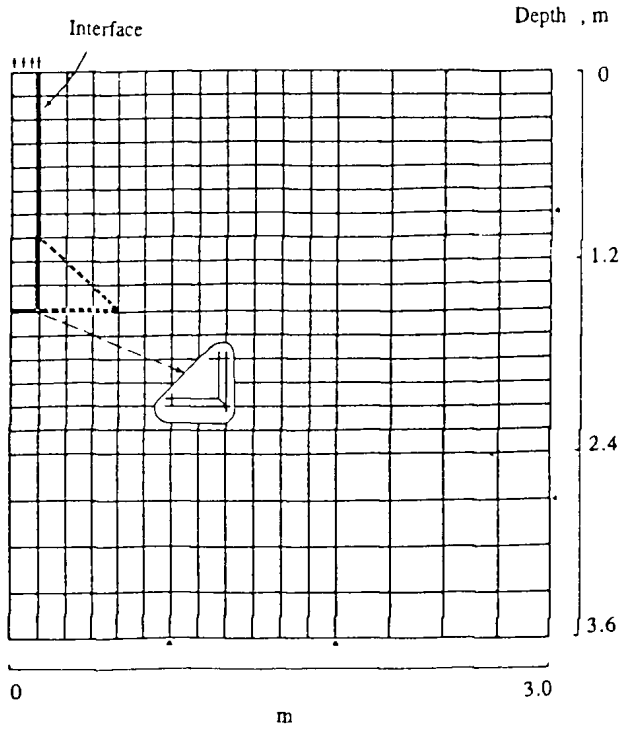

Figure 4. Finite element mesh for straight and belled shafts

shaft was reached at K= 10^7.

Straight Shaft:

Variation of normal stresses along the straight shaft are shown in Figure 5(a). Results show that a greater normal stress is developed by increasing the magnitude of pullout load. this could be the reuslt of stiffening the interface material. Pronounced load distribution takes place in the soil and in the shaft. Figure 5(b) shows the shear stress

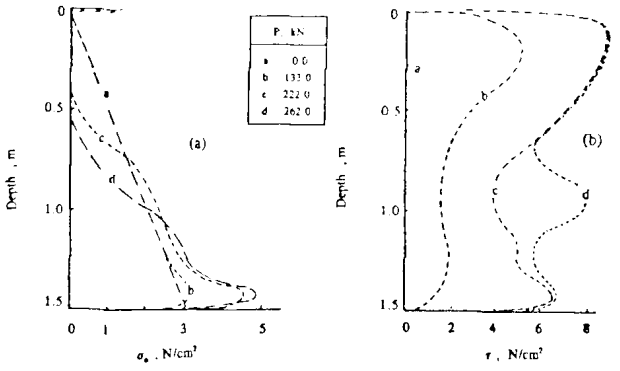

Figure 5(a). Normal stress distribution along straight shaft
Figure 5(b). Shear stress distribution along straight shaft

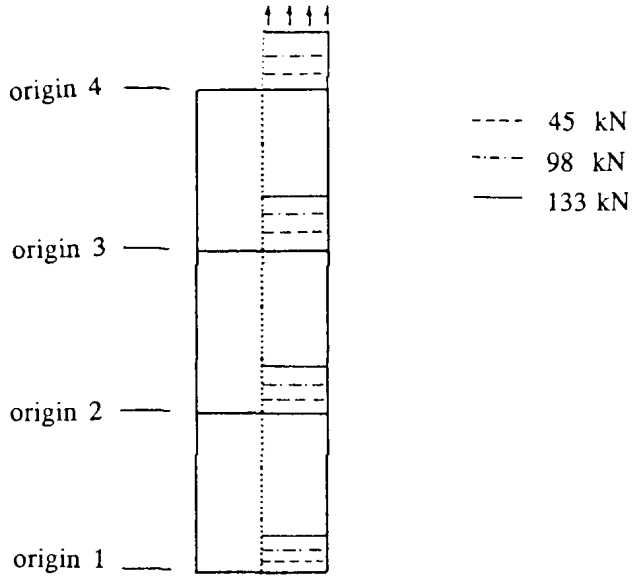

Figure 6. distortion of straight shaft under tension

variation along the straight shaft. The maximum shear stress occurs near the top of the shaft.

A schematic representation of the distortion of the shaft during three stages of loading is shown in Figure 6. Each data point constitutes a load increment. A higher displacement is observed at the top of the shaft than at its tip. This is due to the shaft elongation under tension.

Belled Shaft:

A schematic representation of the distortion of the belled shaft in three stages of loading is given in Figure 7.

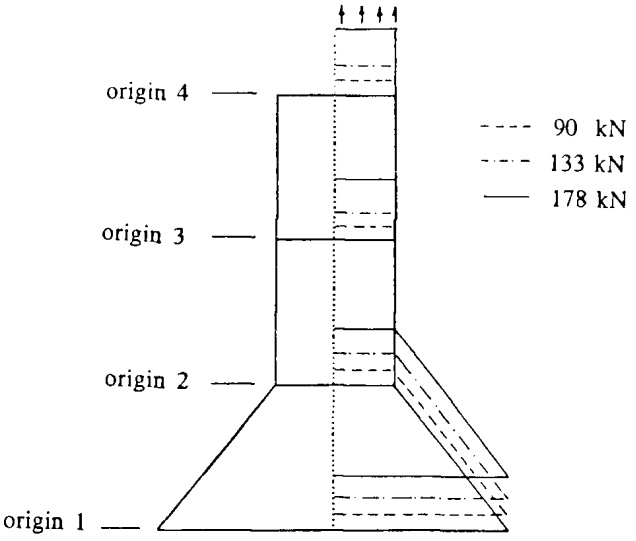

Figure 7. Distortion of belled shaft under tension

Each data point represents a load increment. Variation of normal stresses along the belled shaft are given in Figure 8(a). The maximum normal stress in this case appears at the depth of 1.05m, which is at the neck of the bell. Figure 8(b) shows the variation of shear stresses along the belled shaft; pronounced distribution of stresses are also apparent in this case.

Figure 9 shows the state of stress in the vicinity of the belled shaft at the maximum pullout load capacity. The maximum shear stress occurs at the bell vicinity of the shaft and at the tip of the bell. Large values of shear stresses appear also in the soil zone beneath the shaft, which could be the result of assuming a large value for the stiffness modulus for the interface elements at the tip of the shaft (E= 5 × 108 N/cm^2). This large value was being used to prevent a crack from opening between the soil and tip of the shaft.

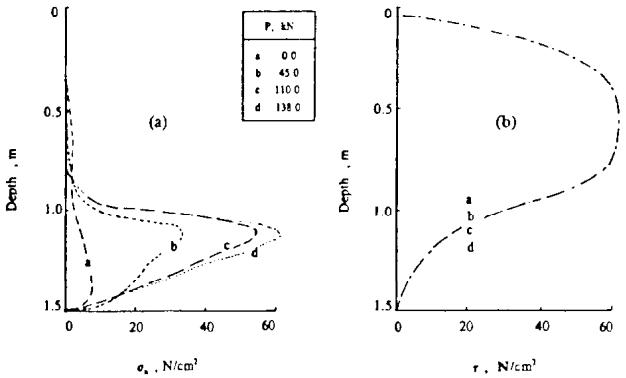

Figure 8 (a). Normal stress distribution along belled shaft
Figure 8(b). Shear stress distribution along belled shaft

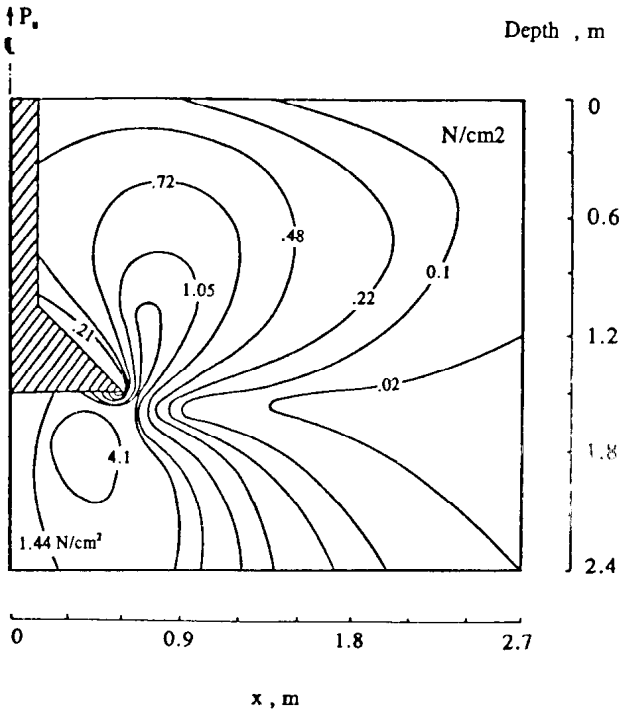

Figure 9. Lines of equal shear stress along belled shaft at P_u= 263N

Ultimate Load Analysis

For the purpose of comparison with the results obtained in the finite element analysis, the straight and belled anchor shafts were analyzed by conventional methods, and approximate values of ultimate uplift of anchors were computed.

Conventional methods of analysis basically fall into three categories [2,3]: cylindrical strength method, cone-of-earth method and Balla et al. or curved surface method. The first two methods were used in this paper to compute the ultimate uplift load capacity of the anchor shafts.

The results of maximum uplift force Q_u obtained by conventional methods are shown in Table 2. The soil cohesion factor in the analysis is taken as 4.8 N/cm^2.

TABLE 2. Ultimate Pullout Load Capacity computed by Closed Form Conventional and Finite Element Methods

Method	Straight Shaft	BelledShaft Q_u, kN
Cylindrical Strength	74.7	330.1
Cone-of-Earth, θ= 60°	371.9	711.3
Cone-of-Earth, θ= 42.5	834.0	1283.8
Finite Element	137.9	262.4

CONCLUSIONS

The main conclusions from the study are:

1- Smaller displacements occur in the belled anchor

shaft than in the straight shaft, when both are subjected to the same amount of pullout force. The pullout resistance of the straight shaft is about 50% of that of the belled shaft, which is a feature that should be considered when economic factors are important.

2- With some limitations, the finite element method of analysis presented in this paper, estimated the magnitude and direction of stresses and displacements at any stage of loading, which may assist in finding the failure surface in the soil medium, and also in determining the degree of accuracy of each of the closed form solutions.

3- Some difficulties appear in using the interface elements in this particular finite element program. Realistic use of interface elements require a great deal of assumptions and approximations in the input data. These difficulties are due to the tension forces in the soil and interface elements.

4- The coefficient COEF used in scaling the interface element's shear stiffness has a pronounced influence on the soil-structure interaction behaviour.

NOMENCLATURE

E_c, E_s	Young's modulus of concrete and soil
E_i, E_t	Initial and tangent modulus
K_0	Coefficient of earth pressure at rest
K_{nn}, K_{sn}, K_{ss}	Stiffness coefficients in normal, cross shear-normal and shear directions
P	Applied load
Q_u	Ultimate uplift force
R_f	Failure ratio
u,v	Displacement components in x and y directions
θ	Angle between failure plane and horizontal surface
ϕ	Angle of internal friction
γ_c, γ_s	Unit weight of concrete and soil
ε	Strain
ν_c, ν_s	Poison ratio of concrete and soil
σ_i	Principal stress at a point (i= 1,2,3)
τ	Shear stress

REFERENCES

1. C.S.Ladd and R.B. Boovee: Consolidated undrained plane strain shear tests on Boston blue clay, U.S. Army Material Command, Project No. 1-V-0-14501-B-52A-01, Vicksbure, Miss. (1971).
2. F.H. Kulhawy, and D.W. Korzera: Uplift testing on Modeled Drilled Shafts in Sands, Jr. Geotech. Engr. Div., *ASCE*, Vol. 105, No. GT1, (1979).
3. G.S. Jain: A comparative study of multi-underreamed pile with large diameter pile in sandy soil, Proc. 3rd Budapest Conf. on Soil Mechanics and Foundations, (1968).
4. S.S. Rao: "*The Finite Element Method in Engineering*," Pergamon Press, (1989).
5. E. Hinton: "*Recent Advances in Non-Linear Computational Mechanics*," Pineridge Press, Swansea, U.K., (1982).
6. J.M. Horner: Vertical Uplift Tests on Model Straight and Belled Auger Footings, Bureau of Reclamation, REC-CRC 72-16, Springfield, VA, (1978).
7. Universal Anchorage Company: "*Ground Anchors Manual*", Universal Anchorage Company, Lancashire, U.K.